Journal of Crystal Growth ∎ (∎∎∎∎) ∎∎∎–∎∎∎

Contents lists available at ScienceDirect

Journal of Crystal Growth

journal homepage: www.elsevier.com/locate/jcrysgro

Sensitivity of quantum cascade laser performance to thickness and doping variations ☆

D.F. Siriani [a,*], C.A. Wang [a], J.P. Donnelly [a], M.K. Connors [a], L.J. Missaggia [a], D.R. Calawa [a], D. McNulty [a], M.C. Zheng [a], T.S. Mansuripur [b], F. Capasso [b]

[a] *Lincoln Laboratory, Massachusetts Institute of Technology, Lexington, MA 02420, USA*
[b] *John A. Paulson School of Engineering and Applied Sciences, Harvard University, Cambridge, MA 02138, USA*

ARTICLE INFO

Keywords:
A3. Metalorganic vapor phase epitaxy
B2. Semiconducting III–V materials
B3. Infrared devices
B3. Quantum cascade lasers

ABSTRACT

We report on a study of the effects of intentional thickness and doping variations on QCL performance. The measured QCL data had very similar trends to those predicted by an in-house QCL model. It was found that absolute changes to the QCL period had a very small effect on emission wavelength (wavelength/period change < 10 nm/Å), whereas the complementary thickness changes between the wells and barriers had a large effect (wavelength/thickness change = 550 nm/Å). The threshold voltage also changed with these variations and generally agreed well with the model. We show through modeling and experiments that intentional structure variations can have largely different magnitudes of effect on QCL performance.

1. Introduction

Quantum cascade lasers (QCLs) [1] are coherent optical sources capable of room temperature, continuous wave operation over a broad bandwidth in the mid-wave infrared (MWIR, 3–7 µm) and long-wave infrared (LWIR, 8–12 µm) wavelength ranges. This aspect makes them appealing for applications in infrared countermeasures, spectroscopy, chemical and biological sensing, and free-space optical communications. The flexible wavelengths of QCLs are achievable because the optical transition energy is determined by the energy separation of subband states in the conduction band of a coupled quantum-well structure. The energy-level separation is determined by the thicknesses of the many quantum wells and barriers in the structure, which typically can number more than 20 layers with some layers only a few monolayers thick. As such, there is potential for unintentional growth variations to produce significant differences between the intended and physically realized QCL structure. For example, a 6% reduction in QCL wavelength from the designed 8.1 µm wavelength has been attributed to a 5% reduction in layer thicknesses [2]. While there have been numerous studies on the growth optimization of QCLs, those studies have focused mainly on growth conditions such as temperature, growth rate, V/III ratio, and growth interrupts [3–8,10].

This work reports the study of the effects of layer thickness and doping variations on the performance of QCLs grown by OMVPE. As explored in other work, OMVPE growth of QCL material in a step-flow growth mode is sensitively dependent on growth conditions, many of which can affect the actual as-grown QCL structure [4,5,7,8]. Different types of thickness changes were intentionally incorporated throughout the QCL structure to understand some potential growth variations, such as effects of evolving or miscalibrated growth rates. Moreover, doping in the injector region and the thickness of the injection barrier were altered to witness their effects on carrier transport. All grown structures were characterized under pulsed conditions; electroluminescence and current–light–voltage data were collected on fabricated mesa structures and ridge lasers, respectively. In order to determine if the growth effects on performance could be predicted, experimental results were compared to calculations from an in-house model. This study shows that different growth variations can have orders of magnitude difference in changes to QCL properties, such as wavelength and current transport.

2. Experimental procedure

The lattice-matched AlInAs/GaInAs QCL structures were grown on (100) InP substrates by organometallic vapor phase epitaxy (OMVPE) in a Veeco D125 multi-wafer reactor. Trimethylaluminum

☆This work is sponsored by the Assistant Secretary of Defense for Research& Engineering under Air Force Contract FA8721-05-C-0002. Opinions, interpretations, conclusions and recommendations are those of the author and are not necessarily endorsed by the United States Government.

* Corresponding author. Tel.: +1 781 981 5858.
E-mail address: dominic.siriani@LL.mit.edu (D.F. Siriani).

http://dx.doi.org/10.1016/j.jcrysgro.2015.11.006
0022-0248/© 2015 Elsevier B.V. All rights reserved.

(TMAl), trimethylindium (TMIn), trimethylgallium (TMGa), phosphine (PH_3), and arsine (AsH_3) were used as precursors and disilane (Si_2H_6) was the n-type dopant, as described previously [9]. H_2 was used as the carrier gas. The growth temperature was 625° C, and the growth rate was ~0.3 nm/s for both AlInAs and GaInAs. The InP cladding was grown at a higher rate of 0.6–0.7 nm/s. No growth interrupts were used. The V/III ratios were ~90 for AlInAs and GaInAs, and ~130 for InP. The structures were characterized by high-resolution x-ray diffraction (HRXRD) to determine the average alloy composition and the QCL period.

A nominal 8.6 μm QCL structure based on single-phonon-continuum transport was used as the baseline [11]. The injector/active region is composed of nominally lattice-matched $Al_{0.48}$ InAs and $Ga_{0.47}$ InAs on InP, and consists of the following layers: **3.8** / 1.5 / **0.9** / 5.3 / **0.8** / 5.2 / **0.9** / 4.8 / **1.6** / 3.7 / **2.2** / 3.0 / **1.8** / 2.8 / **1.9** / 2.7 / **2.0** / 2.6 / **2.5**/ 2.7 / **3.1** / 2.5. The AlInAs barrier layers are in bold print, and the underlined layers are Si-doped injector layers. The injector doping was 8×10^{10} cm^{-2}. The lower and upper InP cladding layer thickness was 3.5 μm, and was Si doped 5×10^{16} cm^{-3}. GaInAs waveguide layers were Si doped 2×10^{16} cm^{-3} and were 0.5 μm thick. A heavily Si-doped ($>5\times10^{18}$ cm^{-3}) plasmon-confinement layer was 0.5 μm thick.

Two separate studies were performed using this structure. In the first, a full QCL structure with a waveguide was grown, and layer thicknesses throughout the entire 35-period structure were changed uniformly. In this case, either the entire period of the QCL was increased or decreased by making all layers thicker or thinner by 5%, or the period was maintained by making complementary changes in the thickness of each barrier and well layers in steps of 0.5 Å. The samples are summarized in Table 1. In this study, the epitaxial material was fabricated into ridge waveguide lasers and mesa structures.

In the second study, a simplified 20-period structure without the waveguide was grown, and only the thickness of the injection barrier (thick barrier separating the injection and active regions) was varied by ±10 Å and/or the doping was changed by $\pm5\times10^{16}$ cm^{-3} from the nominal values of 38 Å and 1.0×10^{17} cm^{-3}, respectively. In particular, injection barrier thickness was varied in order to see the effects on current transport as predicted by resonant tunneling models [12–14]. The samples from this second study are summarized in Table 2; the epitaxial material was fabricated into circular mesa structures.

Standard photolithography and wet etching techniques were used to fabricate ridge lasers and mesa test structures. Ti–Au metallization was used for topside and backside contacts. The ridge lasers were of variable ridge widths from 10 μm to 25 μm in 5 μm steps. These devices were cleaved into 3-mm-long bars and tested as lasers with uncoated facets. The mesa structures had diameter of 200 μm.

The lasers were probe tested in chip form on a temperature-controlled stage held at 15 °C under pulsed operation (100–200 ns pulses at 10 kHz). Using this setup, current–voltage–power characteristics of the QCLs were collected. The mesas from the first study were cleaved in half; wavelength measurements of devices under bias were then taken using a FTIR spectrometer. The mesa from the second study were characterized using a similar pulsed operation setup as for the lasers, but only current–voltage information was gathered.

Table 1
Summary of samples of study 1.

Sample	Designed period (%)	Designed AlInAs/GaInAs (Å)	Measured period (%)
19	0	0/0	0
21	−5	0/0	−3.3
23	0	+1.0/−1.0	+5.0
25	0	+0.5/−0.5	+2.0
27	+5	0/0	+4.0
29	0	−0.5/+0.5	−0.7

Table 2
Summary of samples of study 2.

Sample	Inj. barrier change (Å)	Doping change (cm^{-3})	Measured period (%)
69	0	0	−0.2
70	+10	0	−0.5
78	+10	+5e16	+0.5
79	−10	+5e16	+0.4
80	+10	−5e16	+0.8
81	−10	−5e16	+0.9
82	0	−5e16	−0.2
83	−10	0	−0.5
84	0	0	−1.4
85	0	+5e16	−0.7

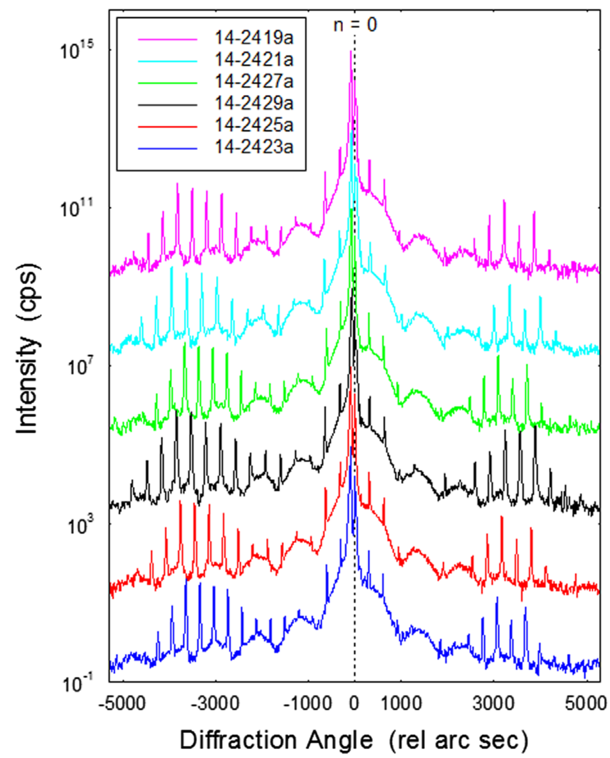

Fig. 1. High-resolution x-ray diffraction of AlInAs/GaInAs QCL structures from Table 1.

3. Results

3.1. Growth summary

High-resolution x-ray diffraction scans for the growths represented in Table 1 are shown in Fig. 1. The sharp satellite peaks and highly resolved interference fringes are indicative of excellent reproducibility of the QCL period. Moreover, the consistent location of the $n=0$ peak is telling of consistent growth from run-to-run and the desired lattice matching. Using the spacing of the satellite peaks in the x-ray data, the actual periods of the QCL structures were deduced. The difference between the measured period and that of the control sample (layer structure given above) are included in the final column of Table 1. The differences between desired and actual period thicknesses are attributed to an increase in growth rate over time due to deposition in the reactor. Similarly, the same measurements were performed for the study 2 growths and measured periods are included in Table 2. In this